

## A COMPREHENSIVE STUDY OF X-RAY EMISSION LINES FROM CATAclySMIC VARIABLES

K.P. Singh<sup>1</sup>, V. R. Rana<sup>1</sup>, E.M. Schlegel<sup>2</sup>, V. Girish<sup>1</sup>, and P.E. Barrett<sup>3</sup>

<sup>1</sup>Tata Institute of Fundamental Research, Mumbai 400005, India

<sup>2</sup>University of Texas, San Antonio, U.S.A.

<sup>3</sup>Johns Hopkins University, Baltimore, MD 21218, U.S.A.

### ABSTRACT

A comprehensive spectral study of a sample of 12 Cataclysmic Variables using high resolution X-ray data from the *Chandra* High Energy Transmission Grating is presented. The G-ratio value for the Fe XXV triplets suggests either coronal or photoionized conditions at 14 MK in U Gem, AO Psc, and one epoch of WX Hyi. For EX Hya it is either coronal plasma at temperatures <1 MK or photoionized plasma at 14 MK that dominates the spectrum. The G-ratio for Si XIII provides a lower limit of  $\sim 10^6$  K for the electron temperature in all objects. SS Cyg and U Gem show significantly broadened emission lines during outburst compared to quiescence corresponding to a high velocity of  $\sim 2300$  km s<sup>-1</sup>. SS Cyg shows a flat-topped line profile for the Fe XXV line that is likely from outflowing wind. Significant broadening of fluorescent Fe line is observed in V603 Aql during its quiescent state. The phase resolved spectroscopy of AM Her shows that the centers of the emission lines of Fe XXVI, S XVI, and the resonance line of Fe XXV are shifted by a few hundred to 1000 km s<sup>-1</sup> from the theoretically expected values indicating bulk motion of ionized matter in the accretion column. Line intensities of H-like ions are modulated by the binary period in EX Hya.

Key words: Cataclysmic Variables; White dwarfs; X-rays:binaries; accretion.

### 1. INTRODUCTION

Cataclysmic Variables (CVs) are short period semi-detached binaries consisting of a white dwarf (WD) primary star accreting via L1 Lagrangian point from a Roche-lobe filling red dwarf main-sequence-like secondary star. CVs can be broadly divided into two main classes, non-magnetic and magnetic. Non-magnetic CVs are further divided into Classical Novae, Recurrent Novae, Dwarf Novae (DN) and Nova-like (NL) variables such as VY Scl and UX UMa. Magnetic CVs consist

of Intermediate Polars (IPs; including DQ Her stars) and Polars (AM Her stars). In non-magnetic CVs, the magnetic field of the WD  $< 10^6$  G (100 T) and accretion takes place through a disk via a boundary layer on the WD. X-ray emission is believed to arise from the boundary layer between the accretion disk and the white dwarf surface. In IPs the magnetic field of the WD is  $\sim 10^6$  G and accretion takes place through a hollowed-out disk and then via accretion columns with the magnetic field controlling the flow in the final stages. Polars are observed to have large ( $\sim 10\%$ ) circular polarization that varies with the orbital period implying a magnetic field  $> 10^7$  G (1000 T). The accretion takes place via a stream outside of the magnetosphere and one or more accretion columns inside the magnetosphere. The infalling material follows the magnetic field lines and approaches a velocity,  $v_{ff} = (2GM/R)^{1/2} = 3600$  km s<sup>-1</sup> as it approaches the WD surface. A standing shock just above the surface converts the kinetic energy into thermal energy, decreasing the velocity by one quarter and increasing the density by four. The material radiates with a maximum temperature of  $\sim 50$  keV in X-rays by cyclotron and bremsstrahlung radiation as it gradually settles on white dwarf surface.

We have analyzed data obtained from the *Chandra* archives for 18 observations of 12 CVs observed with the High Energy Transmission Grating (HETG) onboard the *Chandra* Observatory. There are five DN (SS Cyg, U Gem, WX Hyi, V426 Oph, & SU UMa), one NL (V603 Aql), four IPs (EX Hya, V1223 Sgr, AO Psc & GK Per) and two Polars (AM Her & V834 Cen).

Average spectra of five of the non-magnetic CVs in quiescence have been published previously by others (Mukai et al. (2003), Mauche et al. (2005), Mukai et al. (2005), Szkody et al. (2002), Homer et al. (2004), & Perna et al. (2003)). An early study by Mukai et al. (2003) fitted global models to 7 spectra categorising them into two groups: 'cooling flow' and 'photo-ionized'. Here, we have used line ratios as the diagnostics for the plasma conditions and plasma parameters. In addition, we have studied the line centers, line profiles and line fluxes in the quiescence and outburst states of the CVs and as a function of phase in AM Her and EX Hya. Details will appear

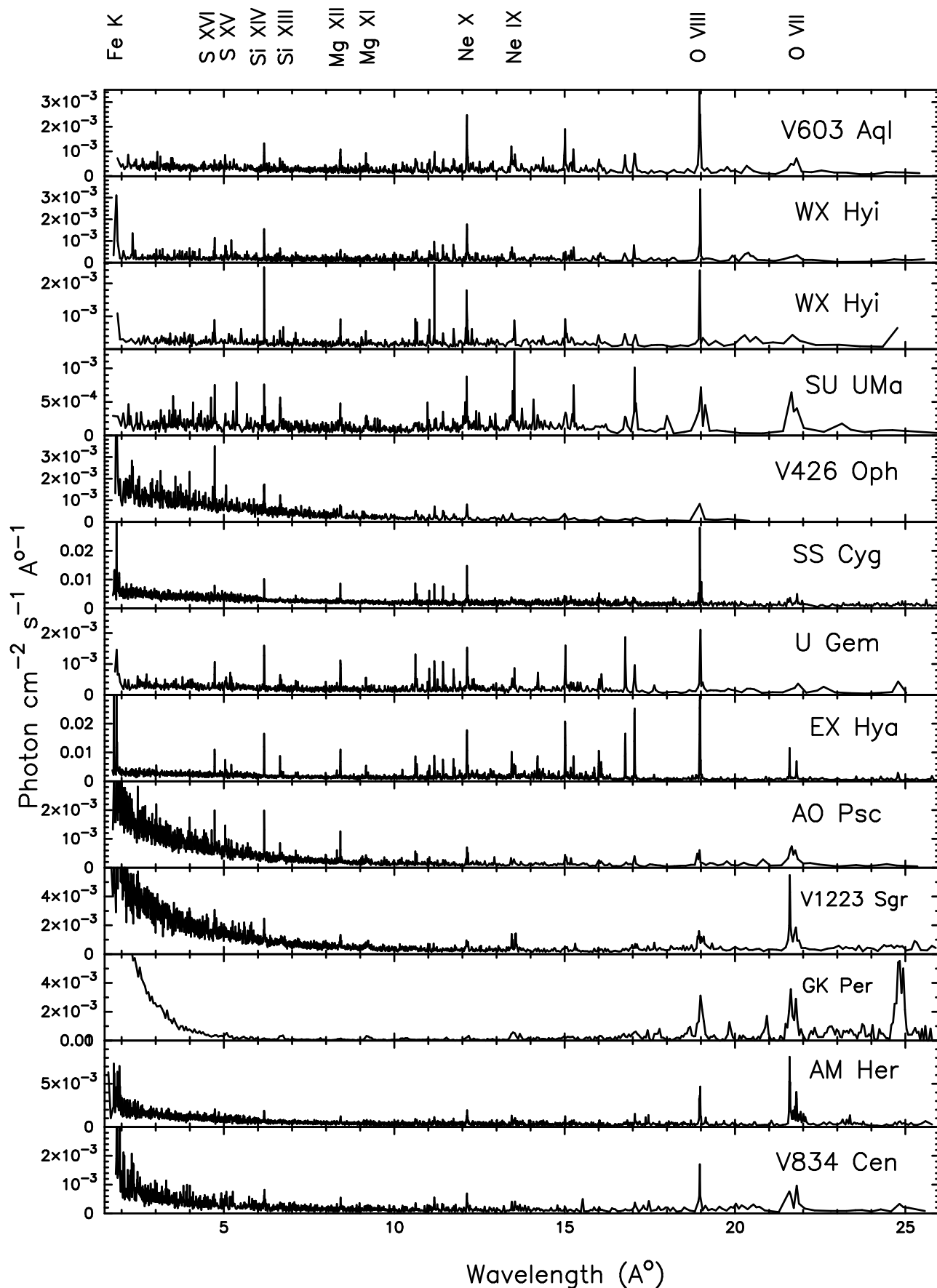


Figure 1. MEG spectra of all CVs in the quiescence state with +1 and -1 orders combined. The H-like and He-like emission lines from O, Ne, Mg, Si, S and Fe K emission lines are labeled.

in Rana et al. (2005), Schlegel et al. (2005) and Girish et al. (2005).

## 2. OBSERVATIONS

The observations were made with the HETG in combination with the Advanced CCD Imaging Spectrometer (ACIS; Garmire et al., 2003) in faint spectroscopy data mode. The HETG consists of the HEG (BW: 1.5–15 Å,  $\Delta E = 0.012$  Å, accuracy of 0.006 Å (abs.), 0.001 Å (rel.)), and the MEG (BW: 2.5–31 Å,  $\Delta E = 0.023$  Å, accuracy of 0.011 Å (abs.), 0.002 Å (rel.)). Most sources were observed during quiescence. SS Cyg and U Gem were also observed during outburst. SS Cyg was observed twice during a short outburst, near the peak of the outburst on 2000 September 12 and during an early decline of a narrow outburst on 2000 September 14. U Gem was observed at the peak of an outburst. AM Her was observed with the Chandra HETG when it was in an intermediate state ( $V_m \sim 14$ ). Observation times ranged from 30–100 ksec.

## 3. ANALYSIS AND RESULTS

The spectra for these sources were extracted using the *Chandra Interactive Analysis of Observations* (CIAO v3.2) and CALDB v3.1. To improve the signal-to-noise ratio, the spectra for the +1 and -1 orders of the HEG and MEG arms were combined together. Several emission lines are seen in the spectra with the principal lines being the  $K\alpha$  lines of Fe XXVI, S XVI, Si XIV, Mg XII, Ne X, and O VIII (all H-like), the triplets (r, i, f) of Fe XXV, S XV, Si XIII, Mg XI, Ne IX, and O VII (all He-like), the Fe XVII lines at 16.78, 17.05 and 17.10 Angstroms (Ne-like), and the Fe I  $K\alpha$  fluorescence. The spectra of all CVs in quiescence along with their identified emission lines are shown in Figure 1. H-like and He-like lines dominate most of the spectra with H-like lines in lower Z ions being stronger. Among the He-like triplets that are resolved, the resonance lines are the most dominant. Strong resonance lines of Fe XXV indicate high temperature ( $> 30$  MK) plasmas (Oelgoetz & Pradhan, 2001). And since no strong redward excess/shift is observed in the resonance lines, the contribution of the dielectronic satellites is probably insignificant.

The spectra are fitted for the continuum using a low order polynomial or a power-law, and Gaussians for the emission lines using XSPEC v11.3. While fitting these models, any broadening in the emission lines (other than instrumental) and possible shift in their positions from the expected values are tested by allowing the line width and center to vary for each line. The line widths are fixed to zero and the line centroids to their expected value, whenever they are found to be consistent with the instrumental resolution and the theoretically expected value. The line fluxes are determined with the 90% confidence. We

have used the C statistic (Nousek & Shue, 1989) to determine the confidence range for each parameter, since it gives better defined limits when using data having a small number of counts per bin. Line ratios R and G can be used for plasma diagnostics if the dielectronic satellites are assumed not to be important. However, density effects and photo-ionization need to be considered.

### 3.1. Plasma diagnostics

In Figure 2 we show the G ratio defined as  $G=(f+i)/r$ , where f, i, and r represent the forbidden, intercombination, and resonance line strengths of the He-like triplet. Given the errors of measurements, the data are not able to clearly indicate whether the coronal or the photoionization models dominate. Somewhat restrictive statements can be made in a few cases, however. For example, based on the G-ratios derived from Fe XXV in U Gem, one epoch of WX Hya, and AO Psc, we have either coronal conditions or photoionized conditions at temperatures  $>10$  MK. In EX Hya it is either coronal plasma at low temperatures  $< 1$  MK or photoionization at  $\sim 14$  MK. From Si XIII, all objects have G values consistent with  $T \geq 10^6$  K. However, the values with the smallest errors are consistent with  $T \geq 10^{6.8}$  K: a temperature at which the coronal and photoionization conditions are inseparable. The errors for the G-values derived from S XV are too large to constrain. Similarly, the values of the R ratio ( $=f/i$ ) indicate high densities. For data with the smallest error bars, we find that  $N_e \geq 10^{16-17} \text{ cm}^{-3}$  for Fe,  $\geq 10^{14} \text{ cm}^{-3}$  for S,  $\geq 10^{13} \text{ cm}^{-3}$  for Si,  $\geq 10^{12} \text{ cm}^{-3}$  for Mg, and  $\geq 10^{11} \text{ cm}^{-3}$  for O.

### 3.2. Fe K line diagnostics for non-magnetic CVs

We have carried out a detailed study of the Fe K lines in the non-magnetic CVs. Hellier & Mukai (2004) have carried out a similar study of the available magnetic CVs. Figure 3 shows the Fe  $K\alpha$  lines for non-magnetic CVs during quiescence along with the best fit model components. Various components of the Fe emission lines are marked. The resonance line is stronger as compared to the other two components of Fe XXV line for all the sources during quiescence, except for SU UMa. The relative strength of r line indicates that the temperature of the emitting plasma is above  $3 \times 10^7$  K (Oelgoetz & Pradhan, 2001), where the principal lines dominate. Therefore, we can use these lines to infer the temperature and density of the emitting region. The G-ratio is very close to 1 (within 90% confidence limit) for all sources, indicating that the plasma is mainly in collisional ionization equilibrium (Oelgoetz & Pradhan, 2001) with electron temperatures  $T_e \geq 10^7$  K for Fe XXV. Only SS Cyg during outburst shows a somewhat higher G-ratio value ( $\sim 2.5$ ) that might indicate the presence of hybrid plasma in the system. However, the lower limit of the 90% confidence interval on G-ratios for SS Cyg during outburst is again very close to unity.

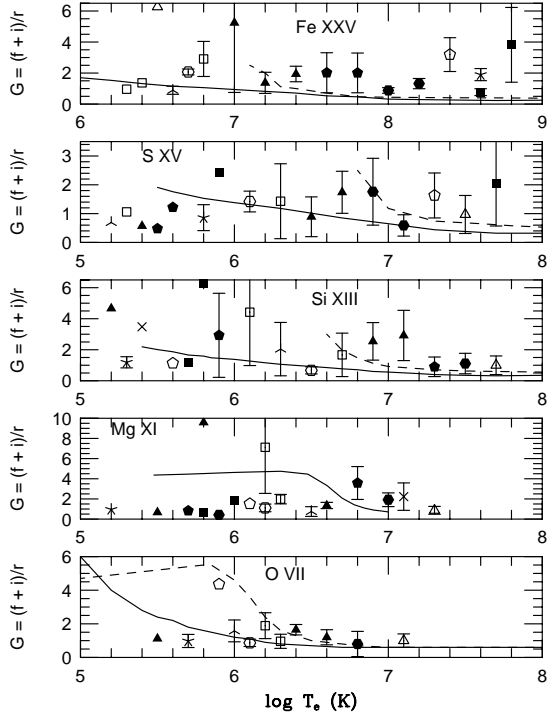


Figure 2. (Top to bottom) The  $G$ -ratios for Fe XXV, S XV, Si XIII, Mg XI and O VII. The curves define the loci of models for coronal (solid) and photoionized (dashed) conditions. The curves are from Bautista & Kallman (2000). Filled-in symbols are DN, star symbol is for AM Her, other starred symbols are for pure IPs, open symbols represent dual objects like DN+IP, Classical Novae+IP etc.

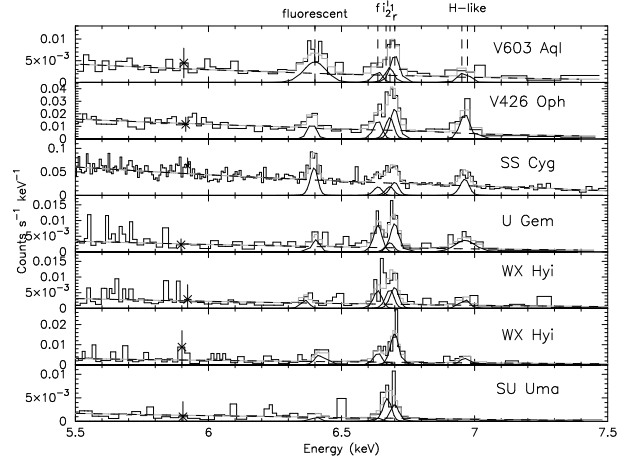


Figure 3. *Chandra* HEG spectra of non-magnetic CVs during the quiescence showing Fe  $K\alpha$  emission lines. The Gaussian components used to model these lines are also shown.

The mean value of the R-ratio for SS Cyg, V603 Aql, V426 Oph, and WX Hyi (in 2002 July 28) varies between 0 and 2. For the two sources, U Gem and WX Hyi (in 2002 July 25), the R-ratios are essentially unconstrained at the lower limit and also the upper limits are very high. For these values the electron densities could be anywhere in the range of  $10^{15-17} \text{ cm}^{-3}$ , or more, thus not allowing us to constrain the range of plasma densities in the non-magnetic CVs studied here.

### 3.3. Center energies and profiles of Fe K lines

Most of the emission lines are observed to be consistent with the instrumental resolution during quiescence, but broadened during outbursts. In particular, the  $r$ ,  $i$  and  $f$  components of Fe XXV are either broadened or shifted significantly from their expected values (see Fig. 4) during outbursts. The outburst (solid line) and the quiescence (dash-dotted line) spectra of U Gem are shown in the top panel of Fig. 4. The 90% confidence values for the widths ( $\sigma$ ) of  $r$  and  $f$  lines are  $51^{+17}_{-18}$  and  $50^{+20}_{-19}$  eV, respectively, which corresponds to velocities of  $2280^{+770}_{-800}$  and  $2260^{+900}_{-860}$   $\text{km s}^{-1}$ . SS Cyg shows a flat-top line profile and the broadened Gaussian line components do not reproduce the observed line profile (see Fig. 2). Such a profile has been reported for N VII line in O-type star,  $\zeta$  Puppis using *Chandra* HETG data and attributed to small velocity gradient at the larger radii in the outflowing winds in the star (Cassinelli et al., 2001; Kahn et al., 2001). The broad emission lines in the outburst spectra of SS Cyg and U Gem have been previously reported by Mauche et al. (2005).

SS Cyg also shows redshifted Fe fluorescence lines during the two outburst observations. The best fit values of the line center show shifts that correspond to velocities of  $2300^{+980}_{-900}$  and  $2300^{+500}_{-440}$   $\text{km s}^{-1}$  during 2000 Septem-

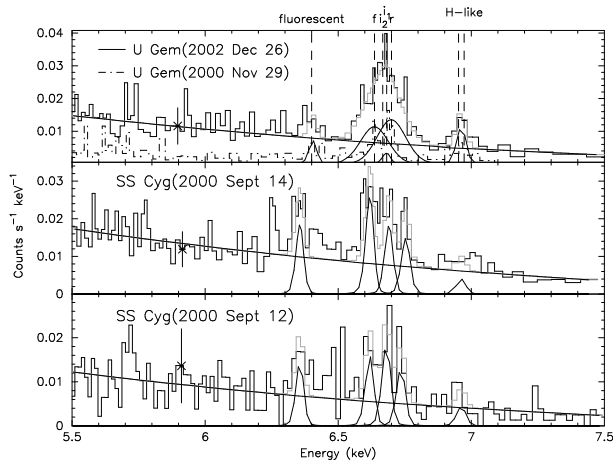


Figure 4. Chandra HEG spectra of U Gem and SS Cyg during the outburst. The dash-dotted curve in the top panel represents the spectrum of U Gem in quiescence. In contrast, the quiescent spectrum of SS Cyg is  $\sim 3$  times brighter.

ber 12 and 14 observations for SS Cyg, respectively. This could be due to a wind flowing away from the system.

The old nova V603 Aql shows a strong fluorescent Fe I line with the highest EW of  $162_{-65}^{+99}$  eV among all sources. The line is also found to be broadened by  $\sim 1700$  km s $^{-1}$ , that is probably due to Doppler broadening or Compton scattering of material in the accretion disk.

### 3.4. Phase resolved X-ray spectroscopy of AM Her

Phase resolved spectra are extracted for five non-overlapping phase bins, each of 0.2 width, by folding data using the well known ephemeris of AM Her. Except for the interval centered around the orbital phase minimum, other intervals had enough counts to estimate the energy and flux of the bright emission lines. The line energies of the Fe XXVI, Fe XXV (r), and S XVI are found to vary as a function of the phase. The most significant shifts are observed in Fe XXVI and are best explained as a sinusoid with semi-amplitude of  $790 \pm 190$  km s $^{-1}$  plus a constant value of  $220 \pm 26$  km s $^{-1}$ . The line shifts in Fe XXV (r), S XVI and Mg XII are consistent with a constant velocity shifts of  $770 \pm 75$  km s $^{-1}$ ,  $500 \pm 160$  km s $^{-1}$ , and  $280 \pm 195$  km s $^{-1}$ , respectively. The presence of a small sinusoid component in them cannot be ruled out, however, as shown in Fig. 5. These modulations indicate bulk motion of ionized matter in the accretion column of AM Her. Based on these velocity shifts and in the framework of the shock model of Aizu (1973) (see also Terada et al., 2001), we infer the temperature, density and height of the line emitting regions in the accretion column. The Fe XXVI ions show velocities that are close to the expected shock velocity for a 0.5 to 0.6  $M_{\odot}$  white dwarf, and modulation due to a single pole accretion.

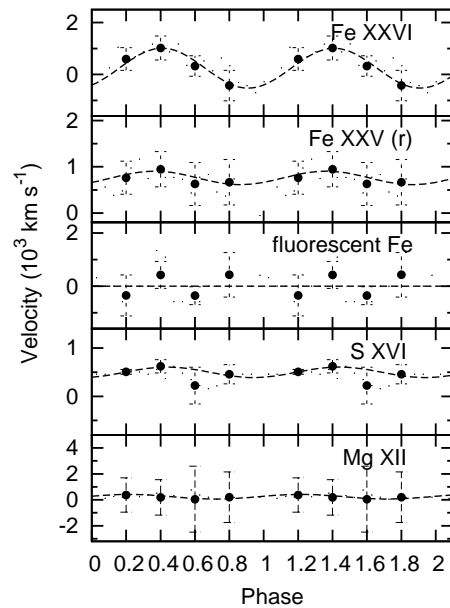


Figure 5. Velocity shifts as a function of orbital phase for the emission lines of Fe XXVI, Fe XXV(r), fluorescent Fe I, S XVI, and Mg XII. The curves show the best fit constant + sinusoidal variation observed.

### 3.5. Phase resolved X-ray spectroscopy of EX Hya

Data for EX Hya are folded using the ephemeris for the binary period as given by Hellier & Sproats (1992), and spectra are extracted for ten non-overlapping phase bins each of 0.1 width. A similar exercise was also done using the spin period of EX Hya. The line fluxes are derived for the principal emission lines observed. In Fig. 6, we show the orbital variation in the line fluxes of H-like emission lines from various ions. A clear phase dependent variation is seen for the O VIII line flux. The Ne X, Mg XII and Si XIV line fluxes show a marginal change over the binary cycle. However, the S XVI and Fe XXVI line fluxes are consistent with being constant over the binary period.

## 4. SUMMARY

Collisionally ionized plasmas appear to dominate the X-ray spectra of several CVs (magnetic as well as non-magnetic). Data are also consistent with photoionization at very high temperatures but present data are not sufficient to make a definitive statement. High densities are required in most CVs. Significant broadening of Fe XXV is seen in U Gem during outburst indicating high velocity gas. Broadening is also seen for fluorescent Fe in V603 Aql during its quiescence state. A broad Fe XXV line with a flat-top profile is seen in SS Cyg in outbursts: high velocity winds or outflows are indicated. Fluorescent Fe line is red-shifted by  $\sim 2300 \pm 500$  km/s in SS Cyg indicating high velocity for fluorescent material during

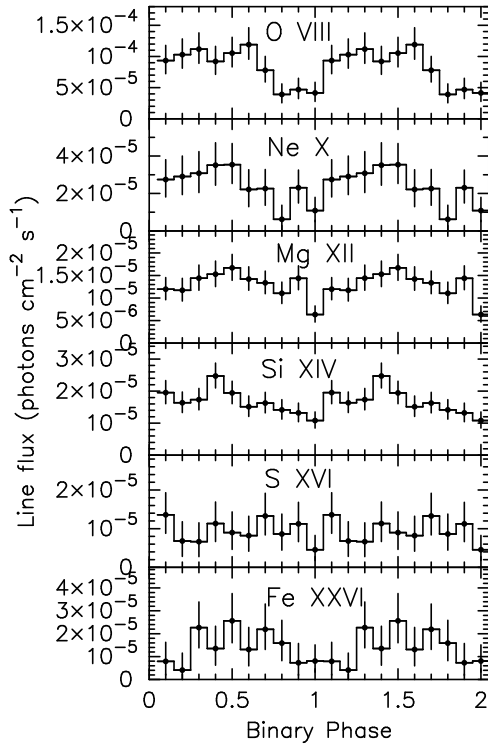


Figure 6. Variation of line fluxes of H-like emission lines from various ions in EX Hya as a function of its orbital phase.

outburst. In AM Her, Fe XXVI line is found to be shifted ( $\sim 1000$  km/s) and modulated at binary period, indicating possible detection of bulk motion in the accretion column. Phase resolved spectroscopy in EX Hya shows binary modulation of line intensity of low Z ions.

## ACKNOWLEDGMENTS

## REFERENCES

- Aizu, K., 1973, Prog. Theor. Phys., 49, 1184
- Bautista, M. A., & Kallman, T. R., 2000, ApJ, 544, 581
- Cassinelli, J. P., Miller, M. A., Waldron, W. L., MacFarlane, J. J., & Cohen, D. H., 2001, ApJ, 554, L55
- Garmire, G. P., Bautz, M. W., Ford, P. G., Nousek, J. A., & Ricker, G. R., Jr. 2003, SPIE, 4851, 28
- Girish, V., Rana, V. R., & Singh, K. P., 2005, ApJ(submitted)
- Hellier, C., & Sproats, L. N., 1992, Inf. Bulletin on Variable Stars, 3724, 1
- Hellier, C., & Mukai, K., 2004, MNRAS, 352, 1037
- Homer, L., et al., 2004, ApJ, 610, 991
- Kahn, S. M., et al., 2001, A&A, 365, L312

Mauche, C. W., Wheatley, P. J., Long, K. S., Raymond, J. C., & Szkody, P. 2005, ASP Conf. series, vol. 330, 355, Eds: J. M. Hameury & J. P. Lasota

Mukai, K., Kinkhabwala, A., Peterson, J. R., Kahn, S. M., & Pearels, F., 2003, ApJ, 586, L77

Mukai, K., & Orio, M., 2005, ApJ, 622, 602

Nousek, J. A., & Shue, D. R. 1989, ApJ, 342, 1207

Oelgoetz, J., & Pradhan, A. K., 2001, MNRAS, 327, L42

Perna, R., McDowell, J., Menou, K., Raymond, J., & Medvedev, M. V., 2003, ApJ, 598, 545

Rana, V. R., Singh, K. P., Schlegel, E. M., & Barrett, P. E., 2005, ApJ(submitted)

Schlegel, E. M., Rana, V. R., V. Girish, Singh, K. P., & Barrett, P. E., 2005 (in preparation)

Szkody, P., Nishikida, K., Raymond, J. C., Seth, A., Hoard, D. W., Long, K., & Sion, E. M., 2002, ApJ, 574, 942

Terada, Y., Ishida, M., Makishima, K., Imanari, T., Fujimoto, R., Matsuzaki, K., & Kaneda, H., 2001, MNRAS, 328, 112